A NOVEL DEEP LEARNING METHOD FOR PNEUMONIA RECOGNITION BASED ON X-RAY IMAGES

Yidong ZHOU[1]

Accurate recognition of different types of pneumonia can assist physicians in providing timely and appropriate treatment. With the progress in computer vision technologies, using convolutional neural networks (CNNs) for the recognition of pulmonary X-ray images has emerged as a key area of research. However, CNNs often involve lots of parameters during training. Additionally, the uneven grayscale distribution and complex structure of pulmonary X-ray images present challenges in image resolution. In this work, we introduce a novel method for pneumonia recognition. ShuffleNetV1 is a lightweight CNN that efficiently extracts image features with a minimal parameter count. We proposed Improved ShuffleNetV1. Specifically, we incorporated the squeeze-and-excitation block (SE block) into the transfer learning-based ShuffleNetV1. This enhancement strengthens the network's capability to recalibrate features, improving its ability to capture critical information. Experimental results demonstrate that Improved ShuffleNetV1 achieves the highest classification accuracy of 86.50%. Our proposed method offers an effective approach for pneumonia recognition.

Keywords: Pneumonia recognition; Deep learning; X-ray images; Convolutional neural network

1. Introduction

Pneumonia is a form of lung infection involving inflammation of the alveoli, typically caused by viruses, bacteria, or fungi[1]. This condition leads to the filling of alveoli with fluid or pus, impairing the efficiency of oxygen exchange. Early recognition and treatment of pneumonia are crucial, as they can significantly reduce the mortality rate of the disease, particularly among children and the elderly[2, 3]. Furthermore, accurately identifying various types of pneumonia is crucial for preventing the spread of the disease.

Traditionally, the diagnosis of pneumonia relies on clinical symptoms, auscultation, and medical imaging, primarily chest X-rays[4]. Chest X-rays can reveal pulmonary shadows and other abnormalities[5], but these signs often lack specificity and can be confused with other pulmonary diseases. Furthermore, the interpretation of X-ray images is highly dependent on the experience and

[1] The Fourth School of Clinical Medicine, Zhejiang Chinese Medical University, Hangzhou, Zhejiang 310053, China

judgment of radiologists, which can lead to subjectivity and variability in diagnoses.

Automated pneumonia recognition using X-ray images can greatly enhance the speed and accuracy of diagnosis[6]. By leveraging deep learning technologies, especially convolutional neural networks (CNNs), pathological features can be automatically identified from images[7], reducing reliance on expert interpretation. This not only speeds up the diagnostic process but also improves the consistency of diagnoses across different healthcare settings, especially in resource-limited environments.

CNNs, through their automated learning of spatial hierarchical features, have been widely applied in various domains, including food supervision[8, 9], facial recognition[10, 11], and autonomous driving[12, 13]. Their robust feature extraction capabilities make CNNs an ideal choice for medical image analysis. Using CNNs for pneumonia recognition based on X-ray images allows for the automatic detection and differentiation of various types of pneumonia. Through training, CNNs are able to recognize complex patterns and subtle changes in images, thus providing accurate support in areas such as medical diagnosis. Learning from large amounts of data, these networks can automatically extract features and perform classification more efficiently and accurately than traditional methods. Numerous studies have already employed CNNs for pneumonia recognition based on X-ray images. For example, Arivoli et al. [14] used a one-dimensional CNN for rapid recognition of COVID-19. Kong et al. [15] combined VGG16 and DenseNet121 for pneumonia recognition. However, these studies often overlook the substantial number of parameters involved in CNN-based image recognition and the impact of key features on pneumonia recognition.

In this study, a transfer learning-based ShuffleNetV1[16] is used to construct Improved ShuffleNetV1. ShuffleNetV1 reduces computational complexity through the use of group convolution and channel shuffle while maintaining network performance. We have incorporated the squeeze-and-excitation block[17] (SE block) into ShuffleNetV1. The SE block directs ShuffleNetV1 to pay more attention to important regions in the image by re-weighting the feature channels and thus performs deeper feature learning in these regions. In this way, the network can capture more detailed and critical information more efficiently, which significantly improves the accuracy of classification or recognition tasks. This enhanced feature representation allows ShuffleNetV1 to perform better when tackling complex visual tasks, distinguishing subtle differences and features more accurately and providing more reliable results. With the introduction of the SE block, ShuffleNetV1 improves not only the computational efficiency, but also the overall performance of the network while maintaining a lightweight architecture.

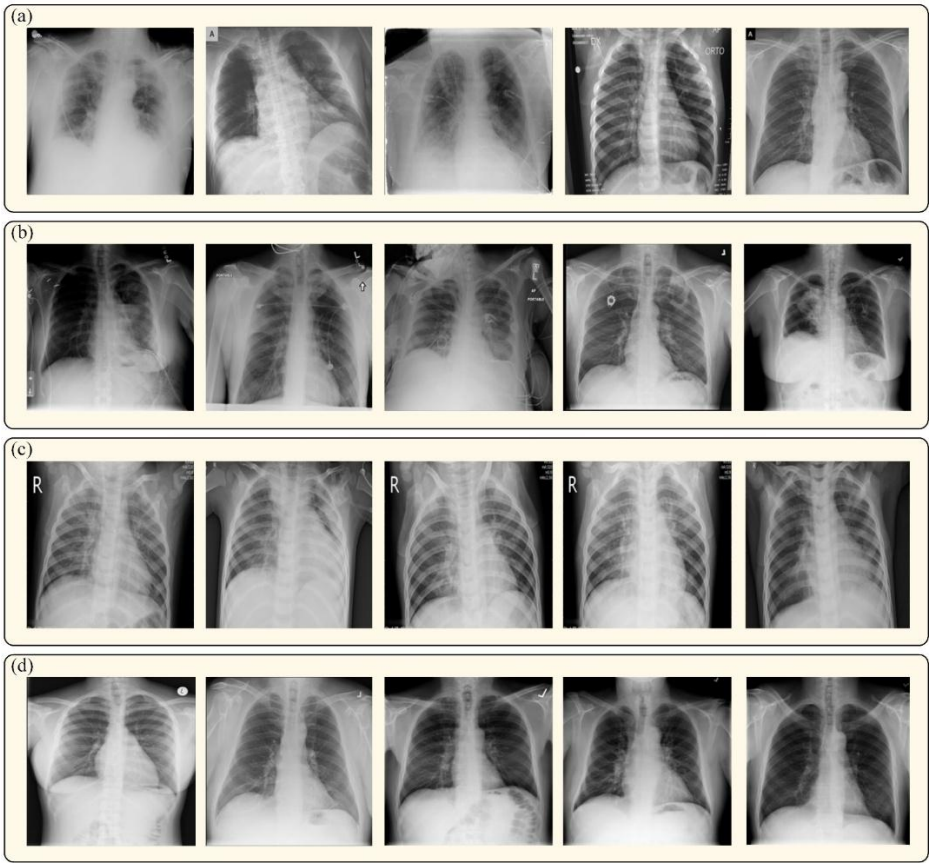

Fig 1. Examples of dataset. (a) Examples of Covid-19. (b) Examples of lung opacity. (c) Examples of viral pneumonia. (d) Examples of Normal.

Table 1

Classes and sample distribution of the dataset.

Classes	Training samples	Testing samples	Total samples
Covid-19	2893	723	3616
Lung opacity	4810	1202	6012
Viral pneumonia	1076	269	1345
Normal	8154	2038	10192

2. Materials and Methods

Dataset

The dataset used in this experiment was sourced from the Kaggle platform (COVID-19 Radiography Database | Kaggle), developed under the guidance of medical experts by a research team from Dhaka University and Qatar University, along with their partners. The dataset comprises chest X-ray images from many

Covid-19 patients, individuals with viral pneumonia, those with pulmonary shadows, and a healthy control group. The sample distribution is detailed in Table 1, while Fig. 1 displays example images. For this study, the dataset was divided for training and testing in an 8:2 ratio. Specifically, it contains 6012 lung opacity samples, 3616 Covid-19 samples, 1345 viral pneumonia samples, and 10192 normal samples. This diverse collection ensures robust model training and evaluation by providing a comprehensive representation of various conditions.

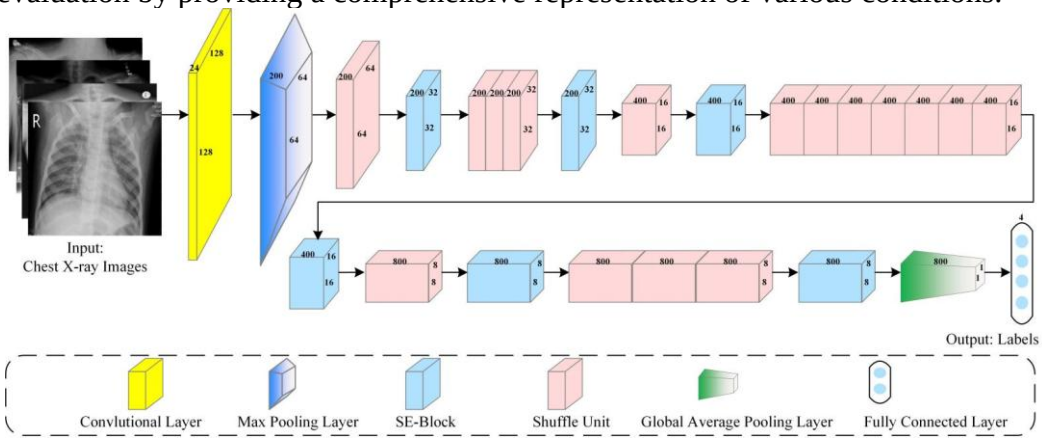

Fig 2. Framework of the proposed method for Covid-19 pneumonia recognition.

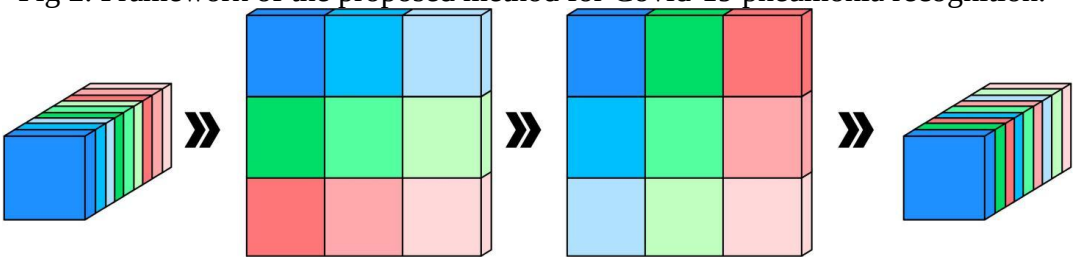

Fig 3. Structure of channel shuffle.

The dataset's rich diversity in medical conditions enhances the model's learning capabilities, allowing it to generalize well across different types of pneumonia and other lung-related diseases. The curated balance between training and testing sets ensures that the model's performance metrics are reliable and indicative of its true capability in a real-world clinical setting.

The inclusion of images from different patient demographics and varying X-ray quality also aids in making the model robust to noise and variations commonly encountered in clinical environments. The use of this dataset aligns with the goal of developing a reliable and efficient diagnostic tool capable of assisting medical professionals in identifying pneumonia and related conditions with high accuracy.

By utilizing this dataset, the study aims to harness the power of deep learning and advanced neural network architectures to advance medical image analysis, ultimately leading to more efficient clinical workflows.

Framework

ShuffleNetV1 significantly reduces the computational burden and number of parameters of the model by using group convolution and channel shuffle techniques. These techniques not only improve the operational efficiency of the model, but also reduce the required computational resources and storage space. Such reduction in computational resource requirements is especially valuable for areas with limited healthcare resources, as it can significantly reduce operational costs and increase the accessibility and ubiquity of medical devices. To further enhance the performance of ShuffleNetV1 in medical image analysis, we developed an improved version of ShuffleNetV1 and applied it to the pneumonia recognition task. The improved architecture, shown in Fig. 2, aims to provide higher recognition accuracy and faster processing speed, thus providing reliable technical support in real clinical applications. This improved version of the model can not only operate efficiently in a limited resource environment, but also play an important role in the early detection of pneumonia, helping doctors to diagnose and treat patients quickly and accurately. Initially, the dataset described in Section II. A is input into the system. ShuffleNetV1 is then enhanced by integrating the SE block to create Improved ShuffleNetV1. The SE block learns the relationships between channels, enabling it to identify which feature channels are important. This enables the network to amplify crucial features while suppressing less important ones, greatly enhancing the model's ability to concentrate on the most relevant parts of the image, thus improving its diagnostic accuracy.

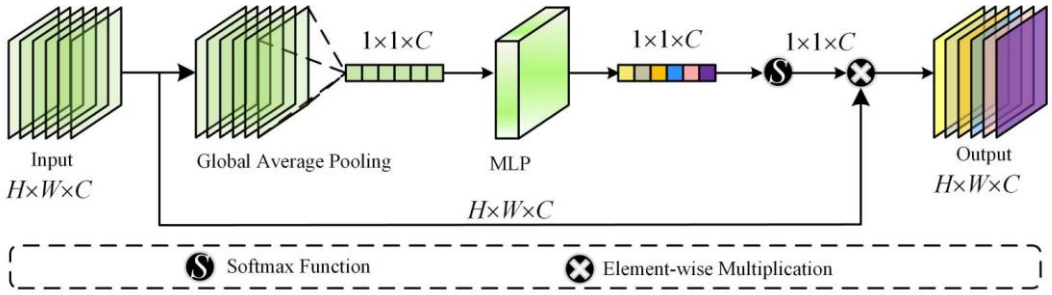

Fig 4. Structure of SE-block.

The architecture includes several essential components: convolutional layers for extracting basic features from chest X-ray images, max pooling layers for reducing the spatial dimensions, thereby making computation more efficient, and SE blocks that adaptively recalibrate channel-wise feature responses

throughout the network. Shuffle units, which employ channel shuffle and group convolutions, are used to enhance the model's efficiency and effectiveness. A global average pooling layer condenses each feature map into a single value, aiding in preventing overfitting and reducing model size. Finally, fully connected layers interpret the extracted features and generate the classification output.

The network outputs labels for four categories: normal, viral pneumonia, lung opacity, and Covid-19. By leveraging the strengths of both ShuffleNetV1 and the SE block, Improved ShuffleNetV1 achieves superior performance in pneumonia recognition compared to traditional models. The advanced architecture not only enhances diagnostic accuracy but also ensures the model remains lightweight and computationally efficient. This balance of performance and efficiency makes Improved ShuffleNetV1 particularly suitable for deployment in diverse clinical settings, including those with limited access to high-end computational resource.

In specific applications, the Improved ShuffleNetV1 is able to quickly and efficiently process medical imaging data to identify different types of pneumonia. This is critical for the early detection and treatment of pneumonia, especially during an epidemic, when early detection and isolation of new crown pneumonia can effectively control the spread of the virus. In addition, the lightweight design of the model means it can be deployed in resource-constrained environments, such as primary hospitals or mobile medical devices, without relying on high-end computing resources.

Overall, the Improved ShuffleNetV1 provides an efficient and reliable pneumonia identification solution for the healthcare industry by finding the optimal balance between computational resources and diagnostic performance. Its superior performance and wide applicability make it a great potential for application around the globe, especially in areas where medical resources are scarce.

Channel Shuffle

Group convolution is an effective technique to reduce the number of parameters in a CNN during construction. Although it significantly lowers computational complexity, this method has a limitation: each output feature map is derived only from its corresponding group of input channels, which restricts the flow of information between different channel groups. However, in some applications, such as X-ray image recognition, capturing the differences between channels can be more crucial than merely capturing spatial features. To address this issue, researchers have introduced the channel shuffle technique. Specifically, this involves manipulating the feature maps produced by the previous layer's group convolution: initially, the feature channels within each group are subdivided into multiple subgroups; these subgroups are then redistributed so that each new group contains subchannels from different groups of the previous layer.

As illustrated in Fig. 3, by transposing and rearranging the order of channels, we can input these shuffled channels into the next layer of the network. This method not only scrambles the original order of channels but also enhances the exchange of information between different channel groups.

SE-block

The attention mechanism can enhance a model's representation of key features[18, 19], which may be particularly useful for distinguishing between different types of pneumonia. The SE block explicitly models the interdependencies between channels to boost the performance of CNNs. Its structure is depicted in Fig. 4. For an input feature map $F \in R^{H \times W \times C}$, where H, W, C represent the height, width, and number of channels, respectively.

Initially, each channel's feature map is compressed into a single scalar by global average pooling (GAP), capturing the global information F_1 of the channel. This process is described as follows:

$$F_1 = GAP(F) \tag{1}$$

Following the GAP, the process involves using a multi-layer perceptron (MLP) followed by a sigmoid activation function to generate importance weights for each channel, denoted as W_1. This MLP typically consists of two layers: the first layer reduces the dimensionality of the input feature vector F_1 from C to C/r (where r is a reduction ratio used to limit the complexity of the model), and the second layer increases the dimensionality back from C/r to C. The sigmoid activation function then maps these transformed features to a range between 0 and 1, representing the importance weights of each channel.

Table 2

Comparison of ShuffleNetV1 and Improved ShuffleNetV1.

Models	Accuracy (%)	Recall (%)	Precision (%)	F1-score (%)
ShuffleNetV1	85.68	84.30	85.02	85.66
Improved ShuffleNetV1	86.50	86.38	85.26	85.92

$$W_1 = Sigmoid(MLP(F_1)) \tag{2}$$

These weights W_1 are specifically used to recalibrate the original feature maps by scaling each channel's activations according to its computed importance. Mathematically, this recalibration is performed using a channel-wise multiplication of the original feature map F and the weights W_1:

$$F_O = F \otimes W_1 \tag{3}$$

Where $\otimes$ represents element-wise multiplication.

Improved ShuffleNetV1

ShuffleNetV1 is a lightweight network designed to maintain high efficiency while delivering adequate performance. The integration of the SE block can further enhance performance without significantly increasing computation. Therefore, we incorporated the SE block into ShuffleNetV1, creating the Improved ShuffleNetV1 for pneumonia recognition based on X-ray images, as illustrated in Fig. 2.

In ShuffleNetV1, the shuffle unit is a unique building block that facilitates lightweight feature extraction through channel shuffle and pointwise group convolution. In Improved ShuffleNetV1, the SE block is added following the shuffle unit. This addition enables the network to capture complex relationships among the high-level features learned by these units, thereby enhancing the model's representational power.

By incorporating the SE block as a separate component within ShuffleNetV1, the network design remains modular, facilitating ease of adjustment and optimization. This modular integration ensures that the enhancements provided by the SE block—namely, the focused recalibration of feature channels based on their relevance—do not compromise the inherent efficiency and lightweight nature of the original ShuffleNetV1 architecture.

3. Experiment

3.1 Experimental Setup

In this work, the experiments are conducted using PyTorch version 2.1.0 on Python 3.6. Input images are uniformly cropped to a resolution of 256×256 pixels. The training process is set for 80 epochs, and the batch size is 32. Loss values are computed using the cross-entropy loss function. The Adam optimizer is used with a learning rate of 0.0001. To thoroughly evaluate the model's performance, multiple metrics are utilized, including F1-score, recall, precision, and accuracy. These metrics collectively provide a comprehensive assessment of the model's ability to classify pneumonia accurately. They take into account not only the correctness of the predictions but also the model's precision and recall capabilities, which are crucial in medical image analysis where both false positives and false negatives have significant consequences.

3.2 Effectiveness of Improved ShuffleNetV1

To validate Improved ShuffleNetV1, we compared it against ShuffleNetV1, with the results displayed in Table 2. The experiment shows that Improved ShuffleNetV1 achieves higher evaluation metrics than ShuffleNetV1, with improvements of 0.82%, 2.08%, 0.24%, and 0.26%, respectively. These improvements are likely attributable to the incorporation of the SE block. Fig. 5 illustrates the performance enhancements of Improved ShuffleNetV1 over the

original ShuffleNetV1 across the training epochs. Both ShuffleNetV1 and Improved ShuffleNetV1 show significant improvements in accuracy over the training period. Improved ShuffleNetV1 demonstrates a consistently higher accuracy compared to ShuffleNetV1, indicating that the improvements made to the model are effective.

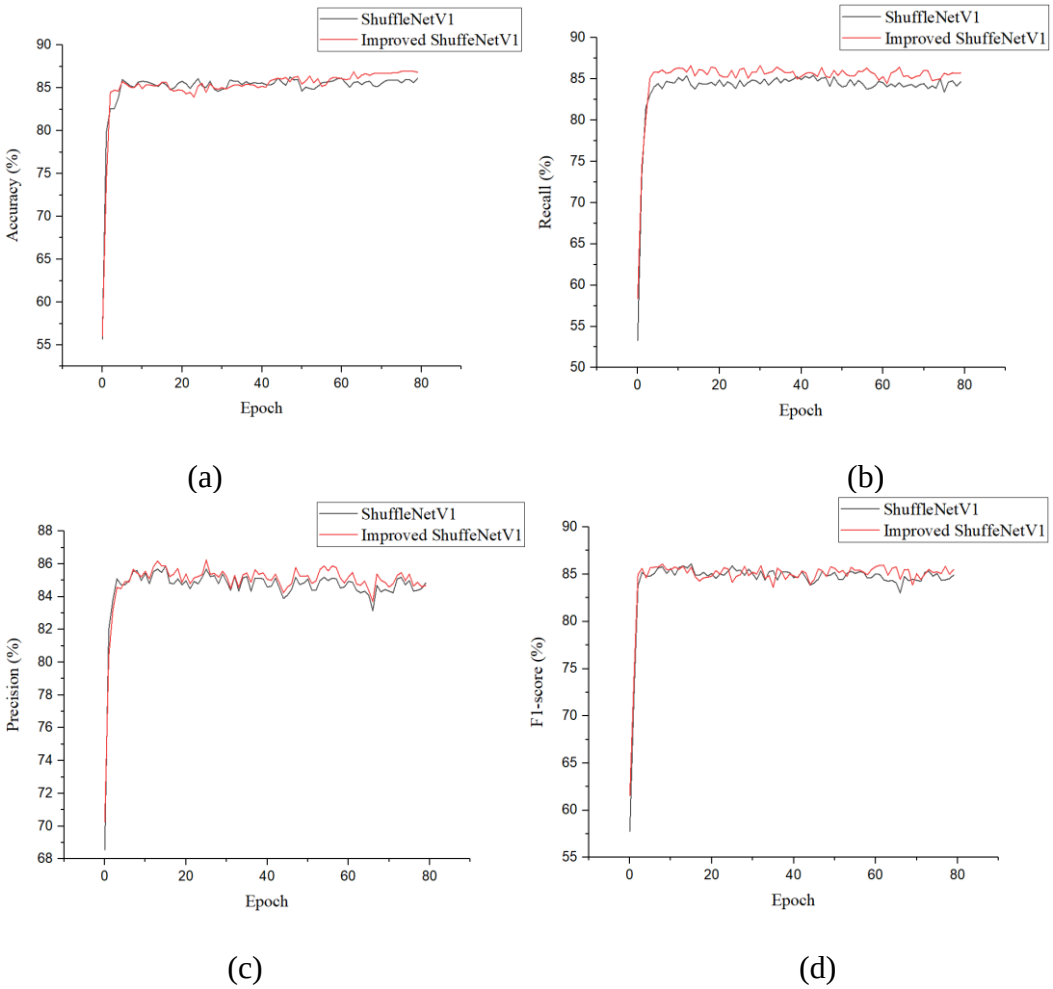

Fig 5. Performance curve of ShuffleNetV1 and Improved ShuffleNetV1. (a) Accuracy curve. (b) Recall curve. (c) Precision curve. (d) F1-score curve.

As shown in Fig. 5(a), the accuracy of Improved ShuffleNetV1 consistently surpasses that of ShuffleNetV1 throughout the training process. Despite some fluctuations between epochs, Improved ShuffleNetV1 ultimately demonstrates more stable and higher accuracy, indicating its enhanced reliability in identifying pneumonia images. From Fig. 5(b), it can be observed that the recall of Improved ShuffleNetV1 is also significantly higher than that of ShuffleNetV1.

This implies that Improved ShuffleNetV1 is better at identifying actual positive cases, i.e., actual pneumonia cases, thereby reducing the chances of missed diagnoses. Fig. 5(c) compares the precision of the two models. Although the precision of both models is close for most of the training period, Improved ShuffleNetV1 generally achieves slightly higher precision than ShuffleNetV1. This indicates that Improved ShuffleNetV1 reduces the false positive rate. Fig. 5(d) shows the variation in the F1-score. The F1-score provides a comprehensive evaluation of the model. Throughout the training process, Improved ShuffleNetV1 consistently exhibits a higher F1-score, indicating its superior balance between recall and precision.

Overall, these improvements in key performance metrics demonstrate the effectiveness of the enhancements made to the model, particularly the incorporation of the SE block. The SE block enhances the model's ability to emphasize useful features and suppress irrelevant ones, making the model more robust to noise, artifacts, and other disruptive factors in X-ray images. By recalibrating the feature maps to focus more on pertinent features, the SE block aids in reducing the influence of misleading information, which can be particularly prevalent in medical imaging. This results in a more reliable and accurate diagnosis, crucial for the effective treatment and management of pneumonia.

Table 3

Multi-model comparison for pneumonia recognition.

Models	Accuracy (%)	Recall (%)	Precision (%)	F1-score (%)
AlexNet	80.55	78.25	86.89	79.20
VGG9	83.24	83.33	85.30	83.56
MobileNetV1	84.48	83.35	86.20	84.80
ResNet18	84.62	84.40	85.28	85.50
Improved ShuffleNetV1	86.50	86.38	85.26	85.92

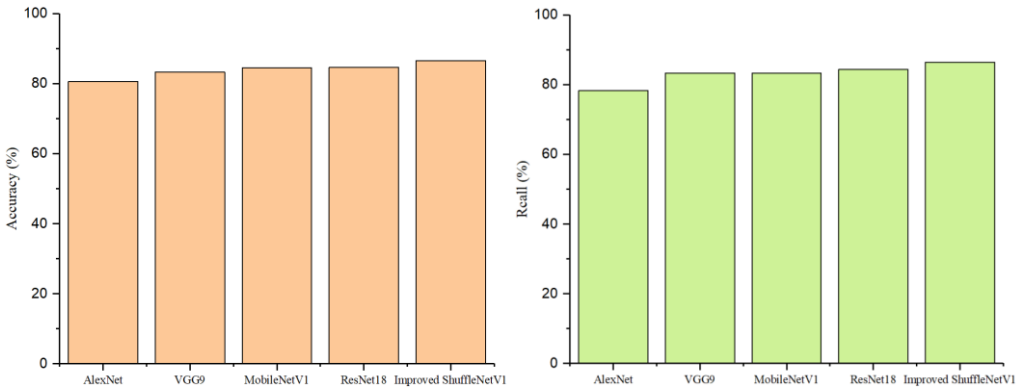

(a) (b)

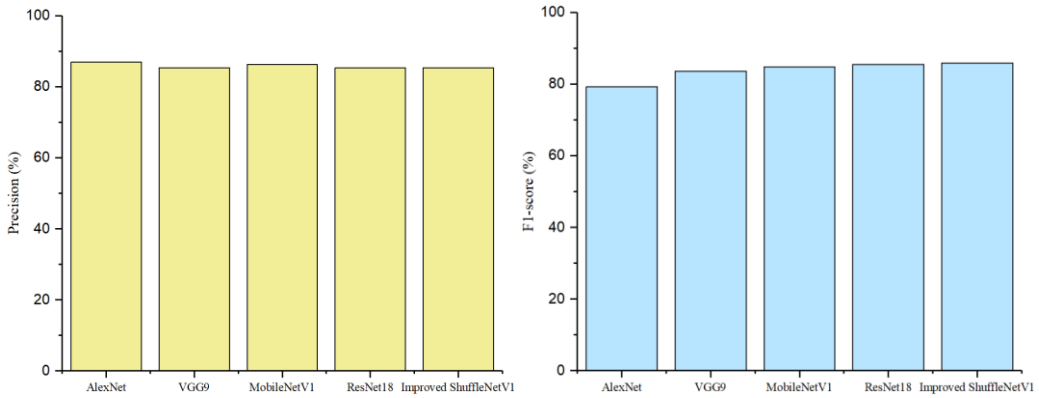

Fig. 6. Histograms for multi-model comparisons. (a) Accuracy, (b) Recall, (c) Precision, (d) F1-score.

3.3 Multi-model Comparison

To thoroughly validate the effectiveness of Improved ShuffleNetV1, we compared it with popular classification CNNs (AlexNet[20], VGG9[21], MobileNetV1[22], and ResNet18[23]). The comparative results are presented in Table 3. The experimental outcomes indicate that Improved ShuffleNetV1 achieved the best classification performance in pneumonia recognition, with an accuracy of 86.50%, recall of 86.38%, precision of 85.26%, and F1-score of 85.50%. These results can be attributed to the channel shuffle technique, which enhances the expressiveness of features, aiding Improved ShuffleNetV1 in better differentiating between healthy and diseased lung tissues.

Furthermore, Fig. 6 illustrates the comparative performance of these models. The histogram clearly shows the distinct advantage of Improved ShuffleNetV1 over AlexNet, VGG9, MobileNetV1, and ResNet18 across all metrics. The visual representation highlights the robustness and effectiveness of Improved ShuffleNetV1 in pneumonia recognition. This makes it particularly valuable for clinical applications where precision and reliability are paramount.

By leveraging advanced techniques like channel shuffle and SE block, Improved ShuffleNetV1 sets a new benchmark in the realm of medical image analysis. The channel shuffle technique allows for more efficient utilization of model parameters, thereby enhancing the model's ability to learn discriminative features from complex medical images. Simultaneously, the SE block ensures that the model focuses on the most critical aspects of the image.

3.4 Comparison with other pneumonia recognition models

To further validate the effectiveness of our network in pneumonia recognition, we reproduced several works that were proposed for pneumonia recognition on X-ray images[24-27]. Chowdhury et.al [24] apply CheXNet to

classify COVID-19, bacterial, and viral pneumonia. Ghose et.al [25] propose a CNN-based deep learning model for automatic COVID-19 detection from chest X-rays. Wang et.al [26] proposes an enhanced DenseNet model with SE-block and max-pooling to improve pneumonia classification. Hussein et.al [27] introduce a lightweight CNN for automatic COVID-19 detection from chest X-ray images. We conducted comparative experiments with these models, and the results are presented in Table 4. Our model demonstrates the best performance among the compared models. The superior performance can be attributed to several key factors. First, the channel shuffle mechanism effectively enhances parameter efficiency, allowing the model to better learn fine-grained and discriminative features from complex pneumonia images. Second, the incorporation of the SE block ensures that the model focuses on the most critical regions of the images, emphasizing the lesion areas associated with pneumonia. Additionally, the lightweight structure of Improved ShuffleNetV1 ensures faster inference times without compromising accuracy, making it a practical solution for real-world medical applications.

Table 4

Comparison with pneumonia recognition models

Models	Accuracy (%)	Recall (%)	Precision (%)	F1-score (%)
Chowdhury et.al [24]	84.96	84.68	84.29	84.02
Ghose et.al [25]	86.00	85.98	85.90	85.26
Wang et.al [26]	84.66	84.60	84.28	83.96
Hussein et.al [27]	85.69	85.72	85.08	85.42
Improved ShuffleNetV1	86.50	86.38	85.26	85.92

4. Conclusion

In this work, we present Improved ShuffleNetV1 for pneumonia recognition based on X-ray images. Improved ShuffleNetV1 enhances the lightweight ShuffleNetV1 by incorporating a channel attention mechanism, the SE block. The SE block explicitly models the dependencies between channels to enhance the network's representational capability. Comparative results with multiple models demonstrate that Improved ShuffleNetV1 achieves the best classification performance, with an accuracy of 86.50%, recall of 86.38%, precision of 85.26%, and F1-score of 85.92%. Our method offers doctors auxiliary imaging diagnostics, improving the accuracy of diagnoses and providing patients with more timely and personalized treatment options, thus reducing the suffering caused by the disease.

Looking ahead, we plan to further investigate how to enhance the model's interpretability, enabling doctors to understand the decision-making process of the model and strengthen their trust in AI-assisted diagnostics. We aim to develop new visualization tools that can display attention maps and show how the model

focuses on specific image areas. This transparency will help bridge the gap between AI outputs and clinical decision-making, fostering a deeper integration of AI in medical practice.

REFERENCES

[1] A. G. Mathioudakis, M. Fally, J. Hansel, R. C. Robey, F. Haseeb et al., "Clinical trials of pneumonia management assess heterogeneous outcomes and measurement instruments," Journal of Clinical Epidemiology, vol. 164, pp. 88-95, 2023.

[2] D. Koulenti, A. Armaganidis, K. Arvaniti, S. Blot, C. Brun-Buisson et al., "Protocol for an international, multicentre, prospective, observational study of nosocomial pneumonia in intensive care units: the PneumoINSPIRE study," Critical Care and Resuscitation, vol. 23, no. 1, pp. 59-66, 2021.

[3] S. P. Bergin, A. Coles, S. B. Calvert, J. Farley, J. H. Powers et al., "PROPHETIC: Prospective Identification of Pneumonia in Hospitalized Patients in the ICU," Chest, vol. 158, no. 6, pp. 2370-2380, 2020.

[4] R. C. Junia and S. K, "Deep learning-based automatic segmentation of COVID-19 in chest X-ray images using ensemble neural net sentinel algorithm," Measurement: Sensors, vol. 33, p. 101117, 2024.

[5] C. C. Ukwuoma, Z. Qin, M. Belal Bin Heyat, F. Akhtar, O. Bamisile et al., "A hybrid explainable ensemble transformer encoder for pneumonia identification from chest X-ray images," Journal of Advanced Research, vol. 48, pp. 191-211, 2023.

[6] D. Verma, C. Bose, N. Tufchi, K. Pant, V. Tripathi et al., "An efficient framework for identification of Tuberculosis and Pneumonia in chest X-ray images using Neural Network," Procedia Computer Science, vol. 171, pp. 217-224, 2020.

[7] S. Liu, L. Wang, and W. Yue, "An efficient medical image classification network based on multi-branch CNN, token grouping Transformer and mixer MLP," Applied Soft Computing, vol. 153, p. 111323, 2024.

[8] W. Min, Z. Wang, J. Yang, C. Liu, and S. Jiang, "Vision-based fruit recognition via multi-scale attention CNN," Computers and Electronics in Agriculture, vol. 210, p. 107911, 2023.

[9] Y. Liu, Y. Zhang, F. Long, J. Bai, Y. Huang et al., "CNN-assisted accurate smartphone testing of μPAD for pork sausage freshness," Journal of Food Engineering, vol. 363, p. 111772, 2024.

[10] L. Goel, N. Debnath, and S. Mundaniya, "A visual question and answering system with support for compound emotions using facial landmark identification with MediaPipe and CNN classifier," Neurocomputing, vol. 588, p. 127623, 2024.

[11] S. Liu, D. Zhao, Z. Sun, and Y. Chen, "BPMB: BayesCNNs with perturbed multi-branch structure for robust facial expression recognition," Image and Vision Computing, vol. 143, p. 104960, 2024.

[12] M. Usman, M. Zaka-Ud-Din, and Q. Ling, "Enhanced encoder–decoder architecture for visual perception multitasking of autonomous driving," Expert Systems with Applications, vol. 246, p. 123249, 2024.

[13] T. Zhao, P. Guo, and Y. Wei, "Road friction estimation based on vision for safe autonomous driving," Mechanical Systems and Signal Processing, vol. 208, p. 111019, 2024.

[14] A. Arivoli, D. Golwala, and R. Reddy, "CoviExpert: COVID-19 detection from chest X-ray using CNN," Measurement: Sensors, vol. 23, p. 100392, 2022.

[15] L. Kong and J. Cheng, "Classification and detection of COVID-19 X-Ray images based on DenseNet and VGG16 feature fusion," Biomedical Signal Processing and Control, vol. 77, p. 103772, 2022.
[16] X. Zhang, X. Zhou, M. Lin, and J. Sun, "ShuffleNet: An Extremely Efficient Convolutional Neural Network for Mobile Devices," in 2018 IEEE/CVF Conference on Computer Vision and Pattern Recognition, 2018, pp. 6848-6856.
[17] J. Hu, L. Shen, and G. Sun, "Squeeze-and-Excitation Networks," in 2018 IEEE/CVF Conference on Computer Vision and Pattern Recognition, 2018, pp. 7132-7141.
[18] C. Qin, D. Qin, Q. Jiang, and B. Zhu, "Forecasting carbon price with attention mechanism and bidirectional long short-term memory network," Energy, vol. 299, p. 131410, 2024.
[19] H. Li, Z. Ma, S.-H. Xiong, Q. Sun, and Z.-S. Chen, "Image-based fire detection using an attention mechanism and pruned dense network transfer learning," Information Sciences, vol. 670, p. 120633, 2024.
[20] A. Krizhevsky, I. Sutskever, and G. E. Hinton, "ImageNet classification with deep convolutional neural networks," Communications of the ACM, vol. 60, pp. 84 - 90, 2012.
[21] S. Liu and W. Deng, "Very deep convolutional neural network based image classification using small training sample size," in 2015 3rd IAPR Asian Conference on Pattern Recognition (ACPR), 2015, pp. 730-734.
[22] A. G. Howard, M. Zhu, B. Chen, D. Kalenichenko, W. Wang et al., "MobileNets: Efficient Convolutional Neural Networks for Mobile Vision Applications," vol. abs/1704.04861, 2017.
[23] K. He, X. Zhang, S. Ren, and J. Sun, "Deep Residual Learning for Image Recognition," in 2016 IEEE Conference on Computer Vision and Pattern Recognition (CVPR), 2016, pp. 770-778.
[24] M. Chowdhury, T. Rahman, A. Khandakar, and S. J. C. S. I. T. Mahmud, "Classification of viral, bacterial, and COVID-19 pneumonia using deep learning framework from chest X-ray images," vol. 12, pp. 1-21, 2022.
[25] P. Ghose, M. A. Uddin, U. K. Acharjee, and S. Sharmin, "Deep viewing for the identification of Covid-19 infection status from chest X-Ray image using CNN based architecture," Intelligent Systems with Applications, vol. 16, p. 200130, 2022.
[26] K. Wang, P. Jiang, J. Meng, and X. Jiang, "Attention-Based DenseNet for Pneumonia Classification," IRBM, vol. 43, no. 5, pp. 479-485, 2022.
[27] H. I. Hussein, A. O. Mohammed, M. M. Hassan, and R. J. Mstafa, "Lightweight deep CNN-based models for early detection of COVID-19 patients from chest X-ray images," Expert Systems with Applications, vol. 223, p. 119900, 2023.